Ultra-low temperature fabrication of copper carbon fibre composites by hydrothermal sintering for heat sinks with enhanced thermal efficiency

Mythili Prakasam, Adrien Morvan, Clio Azina, Loïc Constantin, Graziella Goglio, Alain Largeteau, Sylvie Bourdineaud-Bordère, Jean-Marc Heintz, Yongfeng Lu, Jean-François Silvain

Ultra-low temperature fabrication of copper carbon fibre composites by hydrothermal sintering for heat sinks with enhanced thermal efficiency

Mythili Prakasam[1], Adrien Morvan[1], Clio Azina[1, 2], Loïc Constantin[1, 2], Graziella Goglio[1], Alain Largeteau[1], Sylvie Bordère[3], Jean-Marc Heintz[1], Yongfeng Lu[2], Jean-François Silvain[1, 2]*

[1]Univ. Bordeaux, CNRS, Bordeaux INP, ICMCB, UMR 5026, F-33600 Pessac, France

[2] Department of Electrical Engineering, University of Nebraska – Lincoln, Lincoln, NE, 68588-0511, USA

[3]CNRS, Univ. Bordeaux, Bordeaux INP, I2M, UMR 5295, F-33600 Pessac, France

*Corresponding author : Dr. Jean-François Silvain, ICMCB-CNRS, 87 avenue du Dr. Albert Schweitzer, 33608 Pessac Cedex, France

Email: jean-francois.silvain@icmcb.cnrs.fr

Phone: +33 (0)540008435; Fax: +33 (0)540002761

Graphical abstract:

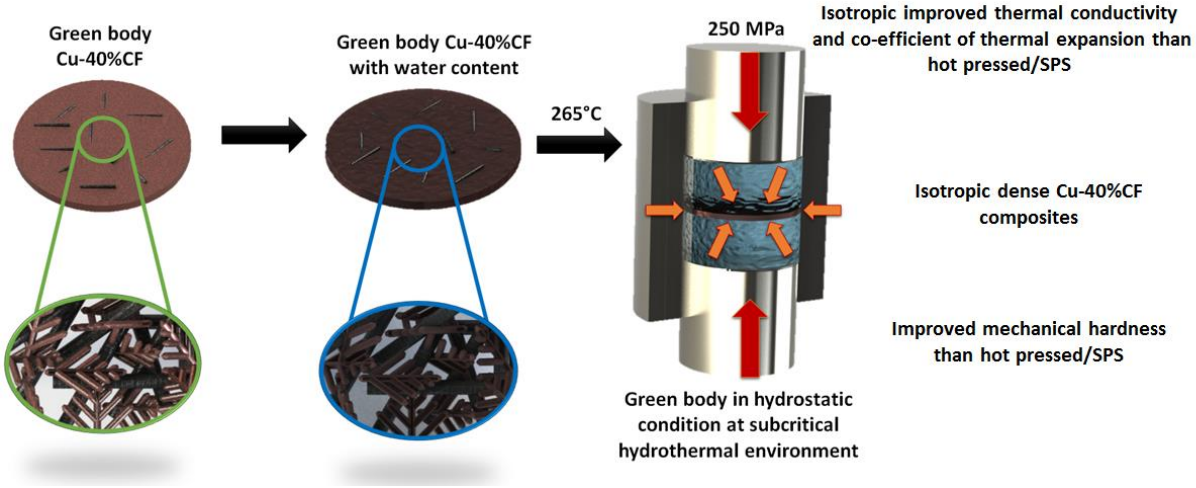

Highlights:

- Dense Cu/40CF composite are fabricated by low temperature hydrothermal sintering at 265 °C and 250 MPa with 5 wt.% water.
- Thermal properties of Cu/40CF composite materials fabricated by low temperature hydrothermal sintering are isotropic

- Hydrothermal sintering increases thermal conductivity and reduces coefficient of thermal expansion in comparison to uniaxial hot pressing
- Hydrothermal sintering improves mechanical hardness of Cu/40CF composite materials in comparison to uniaxial hot pressing

Abstract:

Fabrication of dense Cu/40CF metal matrix composites for heat sink applications by hydrothermal sintering at low temperature (P = 250 MPa; T = 265 °C, t_{sinter} = 60 min; water quantity = 5 wt.%) is reported. Study of various sintering parameters and their influence on densification are investigated. Comparative thermal and microstructural properties of hydrothermally sintered samples with the conventionally used uniaxial hot-pressing samples on Cu/40CF material show considerable improvements, namely increase of thermal conductivity (TC) and decrease of coefficient of thermal expansion (CTE). Hydrothermal sintering yields, through a dissolution/precipitation mechanism, quasi-isotropic thermal properties (TC = 300 W/mK and CTE = 8 10^{-6}/K).

1. Introduction

Heat dissipation in microelectronics and power devices, in optoelectronics and high power diode lasers is an important factor that decides on the reliability, performance and life expectancy of the device [1]. Heat sinks enhance heat dissipation from the hot surface and lowers the thermal barrier between the hot and cold surface (usually atmospheric air). Indeed, owing to the difference in coefficient of thermal expansion (CTE) between the ceramic substrates, heat dissipation materials and semiconductors causes thermal stresses leading to failure at the interface between different layers in devices. Class of materials related to Copper (Cu) and Aluminum (Al) metal matrix composites (MMC) with diverse range of reinforcements are studied for the applications in heat sinks [2,3]. As the aforesaid class of materials have high stiffness at elevated temperatures, low CTE, and high heat dissipation capacity in addition to their lightweight makes it an attractive option for heat sink applications. Carbon fibers (CF) are extensively studied as a reinforcement in MMC due to their excellent mechanical, thermal and electrical properties and negative CTE along the fiber axis. Therefore, Cu/CF MMC are interesting in terms of their thermal conductivity (TC) and electrical conductivity, high wear resistance and low CTE with good machinability and economical price. It has to be noted that the volume fraction of reinforcement can remarkably lower the CTE [4]. However, it will also decrease the final sintered density due to the presence of high-volume concentration of reinforcement. Porosity in the sintered materials acts as a thermal insulator that hinders TC; the sintered material should therefore have density greater than 96% to be employed in heat sinks. Porosity depends on the shape and size of the starting material and also on the sintering parameters such as pressure, temperature, sintering time and the sintering atmosphere. Further, the final properties of the MMCs also depends on the choice of fabrication methodology and homogenous distribution of the reinforcement in the metallic matrix. Fabrication of Cu based MMC are generally made either by liquid (infiltration processes) [5] or solid state sintering [6]. The latter, including sintering by techniques such as hot pressing (HP) [7], is preferred due to the capability to reach high density (even when the volume (vol.) fraction of reinforcement is up to 50 vol.%).

In the present work, we will focus on fabrication of high-density Cu/40 vol.% CF (Cu/40CF) as a prospective heat sink material. The prime difficulty that is encountered during fabrication of Cu/40CF type materials is the absence of chemical reaction and therefore absence of wetting between Copper and Carbon. Various strategies such as coating CF [8-10] prior to

consolidation are employed to compensate the poor wetting between the Cu and CF. HP techniques such as direct, inductive or conventional heated HP and other sintering techniques such as spark plasma sintering (SPS) [11] are used for material consolidation of Cu/40CF through uniaxial pressure. This uniaxial pressure causes preferential orientation/alignment (usually perpendicular to the pressing direction) of the reinforcement, which causes anisotropy in the final composite material properties. High density materials Cu/40CF with isotropic properties can be beneficial in terms of cost cuts (material wastage through shaping and cutting) and for uniform thermal properties with interesting multivalent applications. Various research teams also reported the benefits of low sintering temperatures by SPS (500-550 °C) compared to HP (600-750 °C), resulting in increasing of TC through nanostructuration and rapid sintering time in Cu/CF MMC.

Recently there is a huge upsurge in the research [12-18] on sintering at low temperatures respecting ecological aspects. Hydrothermal sintering [19] meets all these requirements. At ICMCB, we have designed recently a hydro-/ solvothermal sintering apparatus capable of reaching pressure of 350 MPa and temperature of 500 °C to consolidate dense/porous materials and multimaterials [20]. The preliminary results on various materials show a huge promise of this solvent-assisted sintering route on wide spectrum of ceramic and composite materials [21-24] Hydro-/solvothermal sintering is a thermodynamically controlled process consisting of sintering a powder in the presence of a solvent that is externally and mechanically compressed in an autoclave. The main driving force of such a process is the stress gradient within grains induced by external compression leading to the activation of the dissolution/precipitation phenomena at the solid/liquid interface where the reactivity is strongly promoted by hydro- or solvothermal conditions. The solvent is expelled from the sample during densification and recovered in specific spaces for water retreat. Besides its influence on solubility, it acts as a mass transport medium and a pressure transmitting medium.

Hence, in this article, we report on the fabrication of high-density Cu/40CF at low temperature (< 300 °C) using water as solvent by Hydrothermal Sintering (HS). The influence of various relevant parameters in HS sintering on microstructure are investigated. The performance evaluated in terms of their CTE and TC of the fabricated Cu/40CF by HS are compared with the one fabricated by HP.

2. Experimental procedure

2.1 Powder preparation:

The starting powder was made of Cu particles with dendritic shape (Cu-CHL10, Eckart, France), with sizes ranging from 25 µm to 30 µm and pitch type CF (K223HM, Mitsubishi Rayon Co, Japan) with a mean diameter of 10 µm and average lengths ranging between 100 µm to 300 µm. Proper amounts of Cu and CF, corresponding to 60 vol.% Cu and 40% CF were mixed together using a resonant acoustic mixer (Resodyn Labram II), operating at 60 Hz, during 30 s with an acceleration of 100 g_0.

2.2 Hydrothermal sintering

For each experiment, 0.7 g of the starting powder was used for hydrothermal sintering. The experiment was carried out in a metallic (Inconel) autoclave with an inner diameter of 10 mm. The innovative hydrothermal sintering apparatus [20-22] designed at ICMCB has the capability to reach a temperature of 500 °C at a maximum pressure of 350 MPa. This equipment, with unrivalled performances up to date, is versatile to use different solvents and allows to work in acidic, basic and neutral conditions. Pure distilled water was used as a solvent/ reaction medium in hydrothermal sintering (HyS) in the present work. An initial pressure of 125 MPa was applied by using manual hydraulic press at ambient temperature to prevent the water departure as vapor at subsequent heating step. The pressure applied will be released automatically while cooling down to room temperature after sintering. The autoclave being in hydrothermal conditions enables the dissolution and reprecipitation process [20-22]. The thermocouple placed at the proximity of the sample was used to measure the temperature inside the autoclave and an error of ± 10°C has to be considered for the temperature values presented in this study.

Pure distilled water was used as a solvent in hydrothermal sintering (HS). Cu/40CF powders with 5 wt.% of water were charged in the autoclave. An initial pressure P_{start} was applied by using manual hydraulic press at ambient temperature to prevent the water departure as vapor at subsequent heating step. The temperature is then increased up to $T_{sinter.}$ (in the range 100-355 °C) using a heating jacket with a heating rate R_H. When the temperature reaches $T_{sinter.}$, the pressure is increased, in 15 seconds, up to $P_{sinter.}$ (in the range 70-250 MPa). The sample is maintained in the autoclave at $T_{sinter.}$ and $P_{sinter.}$ during $t_{sinter.}$ (in the range 60-180 min). All these sintering experiments are carried out in subcritical water (the temperature is systematically lower that the critical temperature of water, *i.e.* 374.15 °C), Finally, the pressure applied is released automatically while cooling down to room temperature after sintering at a cooling rate R_c. Under the hydrothermal conditions the water is expected to expand and fill the whole

volume of the vessel causing isostatic autogenous pressure. This generated autogenous pressure is dependent on the volume of filling and the quantity of water used. The water is ejected during sintering due to densification and is stored in a specific space destined for water retreat. After the completion of the sintering, the water is expelled totally from the sintered compact.

Heating/cooling rates, sintering time, temperature and pressure, water quantity and relative density of the as-obtained samples are reported in table 2. Some of the samples were precompacted before HS: a cold isostatic pressing (CIP) at 200 MPa bar for a duration of 5 minutes was then applied before sintering, water being added after (sample CC9) or before (sample CC10) CIP. These specific experimental conditions are also mentioned in table 2. The as-sintered samples were polished on both sides.

2.3 Hot pressing

Hot pressing (HP) experiments were done in an in-house built system with heating assisted by induction system. The Cu/40CF powders were compacted in graphitic mold in a vacuum (0.66 Pa) chamber at 650 °C under 50 MPa pressure with sintering time of 20 minutes. The internal of the graphite die was covered with carbon paper (PAPYEX®, Grade N998 with foil thickness of 0.5 mm from M/S. Carbone Lorraine). The heating rate employed was 25 °C/min. The temperature was controlled with a thermocouple inserted inside the mold and close to the composite material.

2.4 Characterization analyses

X-Ray Diffraction (XRD) analysis was performed with a PANalytical X'pert MDP diffractometer with θ-θ Bragg-Brentano configuration with a backscattering graphite monochromator for KαCu radiation working at 40 kV and 40 mA. The density of the sintered composites was measured by the Archimedes' method in distilled water. The microstructure was analyzed by a scanning electron microscope (SEM) (TESCON, VEGA II) on polished and fractured composite surface. The thermal conductivities of the composite materials were calculated using the following equation:

$$K_C = \alpha . \rho_C . C_p$$

where K_C is the TC, α is the thermal diffusivity, ρ_C is the density and C_p is the specific heat of the composite. The thermal diffusivity was measured by the flash laser method (NETZSCH LFA 457, MicroFlash) at 70 °C. Cp values of composite materials were calculated using conventional rule of mixture. The C_p of the CF, and Cu, used in this work, are the following: $C_p(CF) = 838\ J.Kg^{-1}.K^{-1}$ at 70 °C and $C_p(Cu) = 345\ J.Kg^{-1}.K^{-1}$ at 70 °C. For Cu/CF composite materials, due to the anisotropy of the reinforcement, both transverse (parallel to the pressure direction) and in-plane (perpendicular to the pressure direction) thermal diffusivities were measured. The in-plane CTE was measured using a dilatometry equipment (NETZSCH DIL 402, PC), under argon gas flow. Two thermal cycles were performed between room temperature and 250°C with 2°C/min of heating/cooling rate. In order to fulfill electronic industries requirements for heat sink materials, both directions namely parallel to the pressing direction (TC//) and perpendicular to the pressing direction (TC⊥) were calculated whereas just perpendicular CTE (CTE⊥) were measured. Hardness measurements of the Cu/40CF composites were analyzed with Wilson hardness Vickers 452 SVD with a force of 20 N.

3. Results and discussion

The driving force for sintering processes is the stress gradient within grains. Two kinds of stress fields can potentially be involved for HS. The first one is induced by surface tension, leading to tensile stresses at the grain contacts in the range of MPa for micrometer powders. The second one is induced by external pressure that generates high compressive stresses in the range of GPa, for a 200 MPa applied pressure, at the contact zone. Thus, assuming that the driving force induced by external applied pressure dominates, the expected mass transport mechanisms in both the metal phase and the fluid medium can be described according to table 1. Note that the diffusion of copper in the liquid phase is mainly induced by concentration gradient resulting from an increase of solubility when the solid phase is compressed. Compressive stress gradient at the surface of the solid phase thus induces concentration gradient in the liquid phase, which leads to Cu species diffusion and related dissolution/precipitation processes.

Table 1: Expected transport mechanisms in the case where stress field is induced by external uniaxial pressure

Transport location	**Volume of Cu grains**	**Grain surface and interfaces of Cu-Cu and Cu-CF**	**Liquid phase**

Presence of water	No	No	Yes	Yes
Transport mechanism	Thermoplastic deformation	Creep activated by temperature	Creep activated by the presence of water and by temperature	Cu diffusion involving dissolution/ precipitation process

Depending on the experimental sintering conditions, several composites were obtained (see table 2 and Figure 1).

Table 2: Experimental parameters employed in the sintering study of Cu/40CF composites and relative density (R_H: heating rate, R_C: cooling rate)

Sample code	Sintering process	R_H, R_C (°C/min)	Water quantity (wt.%)	Sintering temperature (°C)	Sintering time (min)	P_{start} MPa	Sintering pressure (MPa)	Absolute density (g/cm^3)	Relative density (%)
CC1	HS	5	5	355	180	125	125	5.82	93
CC2	HS	5	5	265	180	125	125	6.19	99
CC3	HS	5	0	265	180	125	125	5.32	85
CC4	HS	5	5	180	180	125	125	5.57	89
CC5	HS	5	5	100	180	125	125	4.13	66
CC6	HS	5	5	265	60	125	125	6.07	97
CC7	HS	5	5	265	60	250	250	4.57	73
CC8	HS	2.5	5	265	60	125	250	6.26	100
CC9*	HS	2.5	5	265	60	125	250	6.26	100
CC10**	HS	2.5	5	265	60	125	250	6.26	100
CC11	HS	5	5	265	60	70	70	5.00	80
CC12	HS	2.5	5	265	480	125	250	6.26	100
HP1	HP	25	0	650	20	30	50	6.01	96

* Cold isostatic pressure (CIP) = 200 MPa for 5 min; **water mixed in sample prior to CIP

It can be seen that full density was reached for, at least, 4 samples that were sintered at a temperature as low as 265 °C. Moreover, no secondary phases were formed in these sintered samples (CC8, 9, 10 and 12) as it can be observed on X ray diffraction patterns (Fig. 1).

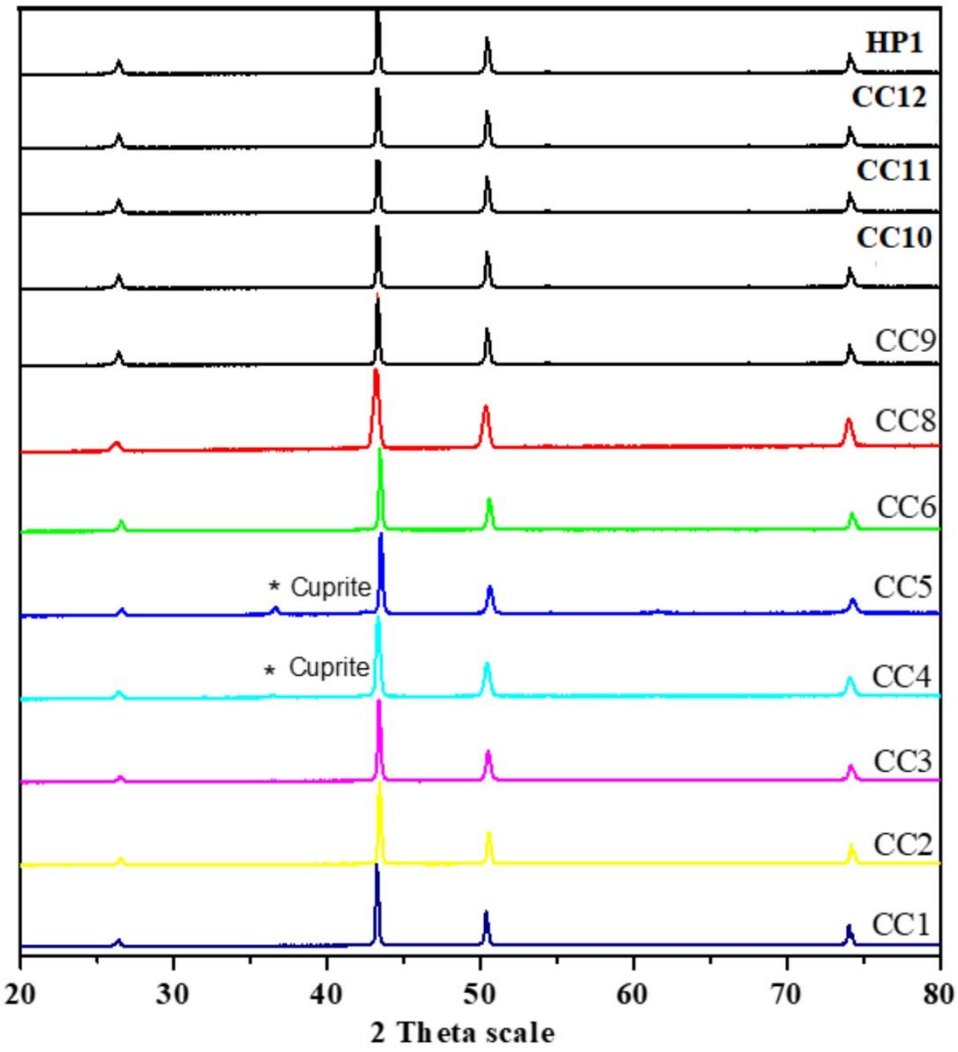

Figure 1: X-ray diffraction patterns of Cu/40CF MMC obtained with different sintering parameters

The influence of the various sintering parameters, presented in table 2, are discussed in detail in the following sections.

3.1 Study of sintering parameters

3.1.1 Role of water

Hydrothermal sintering processes involve water to transport species by dissolving the solid particles in the high compressive stressed region and by precipitating it in the less stressed region. Figures 2 (a) and 2 (b) show the microstructure of Cu/40CF samples sintered at $T_{sinter.}$ = 265 °C during 180 min, with $P_{sinter.}$ = 125 MPa, in absence of water and with 5 wt.% added

water, respectively. It can be observed from Fig. 2 (a) that a lack of water during the pressure-temperature treatment results in the presence of large porosities. Moreover, damaged fibers can be seen inside the larger pores. The pressure applied on the composite powder at 265 °C induces copper grain deformation but also high stress points on CF, leading for some of them to their failure. Conversely, Fig. 2 (b) shows that water induces a uniform microstructure and keeps the carbon fibers unaffected. Presence of water during the sintering clearly increased the density of the sintered sample. Thus, these experiments confirm that the role of water is of first importance for the HS process to obtain dense sintered Cu/40CF MMC at low temperatures. It will be discussed in more details in the sintering effect part.

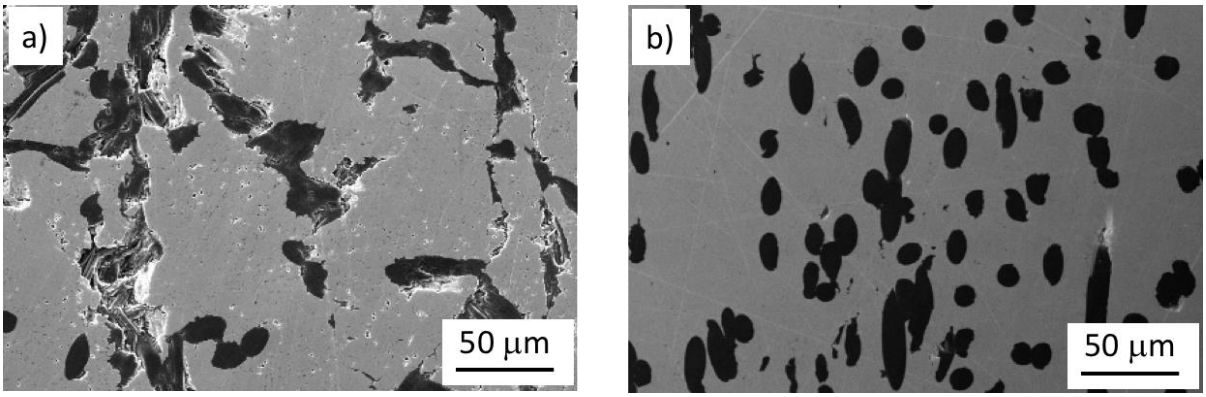

Figure 2. Microstructure of Cu/40CF MMC sintered at 265 °C under 125 MPa (a) without water (CC3) and (b) with 5wt.% of water (CC2)

3.1.2 Influence of the preparation of the green body

Pressure is a major parameter in the compaction of a green body. Cu is known as a ductile metal and therefore application of a pressure on Cu powders can induce plastic deformation and yield solid compacts, even at room temperature. Beside uniaxial pressure, cold isostatic pressure (CIP) may be used to increase the density of the green compact. In the case of our composite powder, this isostatic pressure not only increases metallic contact points but also avoids the preferential orientation of the fibers within the copper matrix, as it can be seen in Fig. 3. The relative density of the green compact after CIP was quite high ($d_{rel.}$ = 65%) due to the probable rearrangement of the copper particles because, at such a pressure, low plastic deformation is expected [25]. Moreover, the CF did not appear affected by the application of the isostatic pressure.

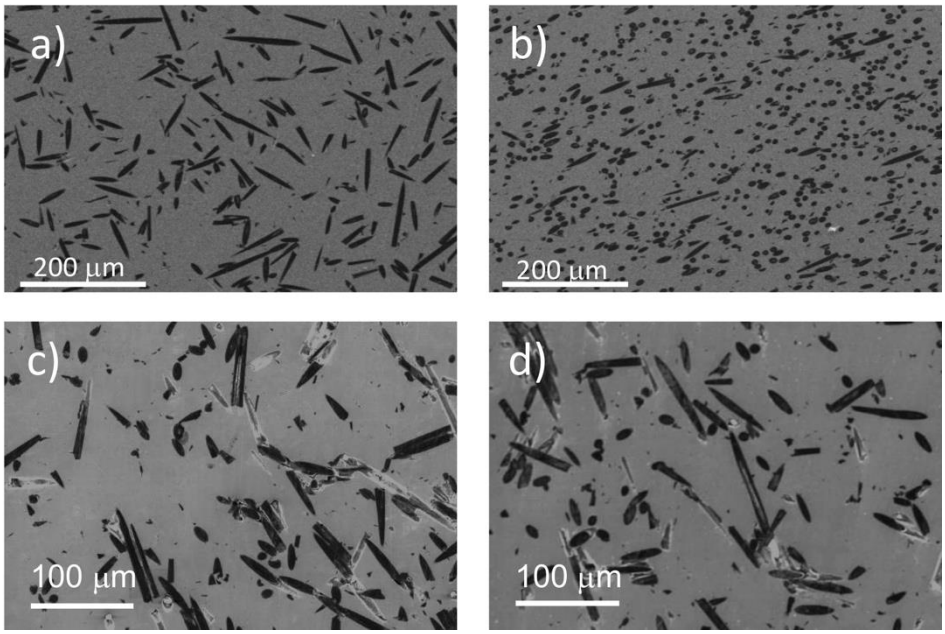

Fig3: SEM micrographs of HP materials a) parallel and b) perpendicular to the pressure direction and HS materials c) parallel and d) perpendicular to the pressure direction

The effect of a CIP pre-compacted step on the hydrothermal densification and on the microstructure of as-sintered Cu/40CF MMC was analyzed with CC8 and CC9 samples. No change of the final density was observed and both samples were fully densified ($d_{rel.}$ = 100%, Table 2). The microstructures were also very close (Fig. 4 (a) and (b)). The way to add water, after or before CIP pre-treatment, was also considered (samples CC9 and CC10, respectively). The densification was complete in both cases ($d_{rel.}$ = 100%).

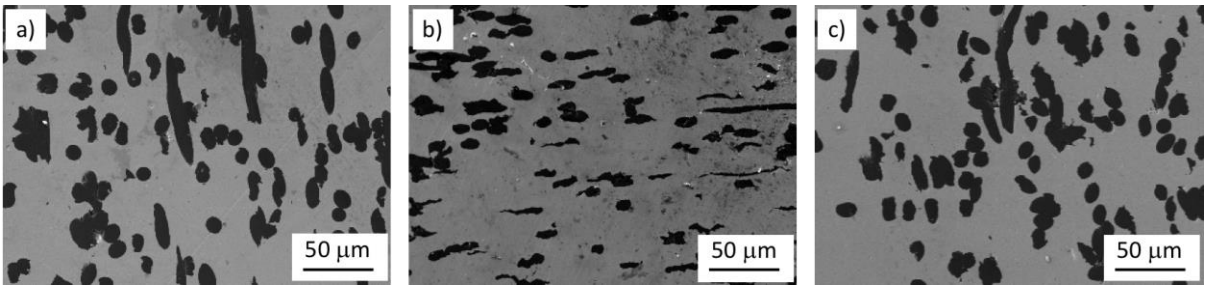

Figure 4: Microstructure of Cu/40CF MMC sintered at 265 °C under 250 MPa with 5 wt.% of water: (a) without CIP of the powder mixture (CC8) (b) with CIP of the powder mixture (CC9) and (c) with CIP of the powder mixture containing water (CC10)

3.1.3 Influence of sintering temperature

Sintering temperature ($T_{sinter.}$) is usually considered as a major parameter for densification whatever the involved sintering route. However, in the case of Cu, A.P. Savitskii et al [26]

reported that high sintering temperatures were not necessary for obtaining dense compacts. Repeated pressing and sintering cycles at low temperature could give Cu samples with hardness and resistance to compression higher than cast Cu. At low temperatures (< 700 °C), densification of Cu took place mainly by plastic deformation and not by atomic diffusion. In our hydrothermal experiments, the effect of the sintering temperatures was investigated in a temperature range where usually no diffusion, nor densification occurred. The results are presented in Fig. 5 (all sintering parameters are given in Table 2). One can note that the sintered density remained low for the lower sintering temperature (100 °C) but then a large increase in density is observed and a maximum of density was obtained for $T_{sinter.}$ = 265 °C. Above that temperature, a decrease of the relative density was observed, although remaining quite high.

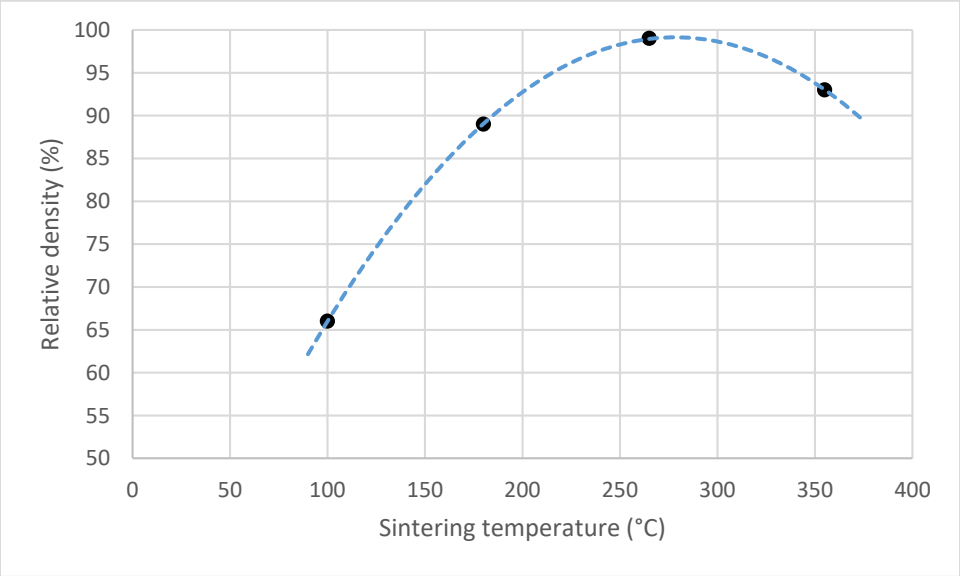

Figure 5: Variation of the relative density of Cu/40CF samples sintered at different temperatures in presence of 5 wt.% of water (R_H=R_C=5 °C.min^{-1}, $t_{sinter.}$ = 180 min., $P_{sinter.}$ = 125 MPa)

As already mentioned, in that sintering temperature range, the combined effect of the temperature and pressure is not sufficient to ensure densification: CC3 experiment sintered at 265 °C and 125 MPa but without added water only reached $d_{rel.}$ = 85%, compared to 99% for the CC2 sample where water was added. In fact, in absence of water in the powder, a 650 °C sintering temperature is needed at 50 MPa to obtain a high final density (HP1 sample, $d_{rel.}$ = 96.3%).

So, the influence of water is clearly pointed out in this hydrothermal sintering process where chemistry plays a large role, even in that low temperature range. Dissolution-precipitation

processes are acting together with plastic deformation to promote densification. Therefore, the question of the dissolution of copper is raised. Theoretically, considering the classical Pourbaix diagram, metallic copper is stable in water [27]. At room temperature, only pH higher than 8 could lead to the formation of Cu_2O (cuprous oxide). In fact, many works have been done on the corrosion of copper by water that shows that this metal is not totally inert in aqueous media [28-30]. Copper can be solubilized in water through the presence of an oxide layer on its surface. For the used Cu powder, no preliminary reduction process was performed before the mixing and sintering steps. Indeed, the presence of a thin oxide layer was proved by XPS measurements. Fig. 6a shows typical XPS spectra, after peak decomposition, the Cu signal (Cu 2p) and Fig. 6b the oxygen signal (O 1s) of dendritic Cu particles. It has to be noticed that the oxygen peaks, located around 531.9 and 530.5 eV, are assigned to $Cu(OH_2)$, OH, H_2O and Cu_2O, CuO, respectively, whereas the Cu peaks located around 932.6 eV and 934.6 eV are assigned to Cu^0 and Cu^{2+} (CuO) respectively. The atomic percent of CuO is lower than 1%.

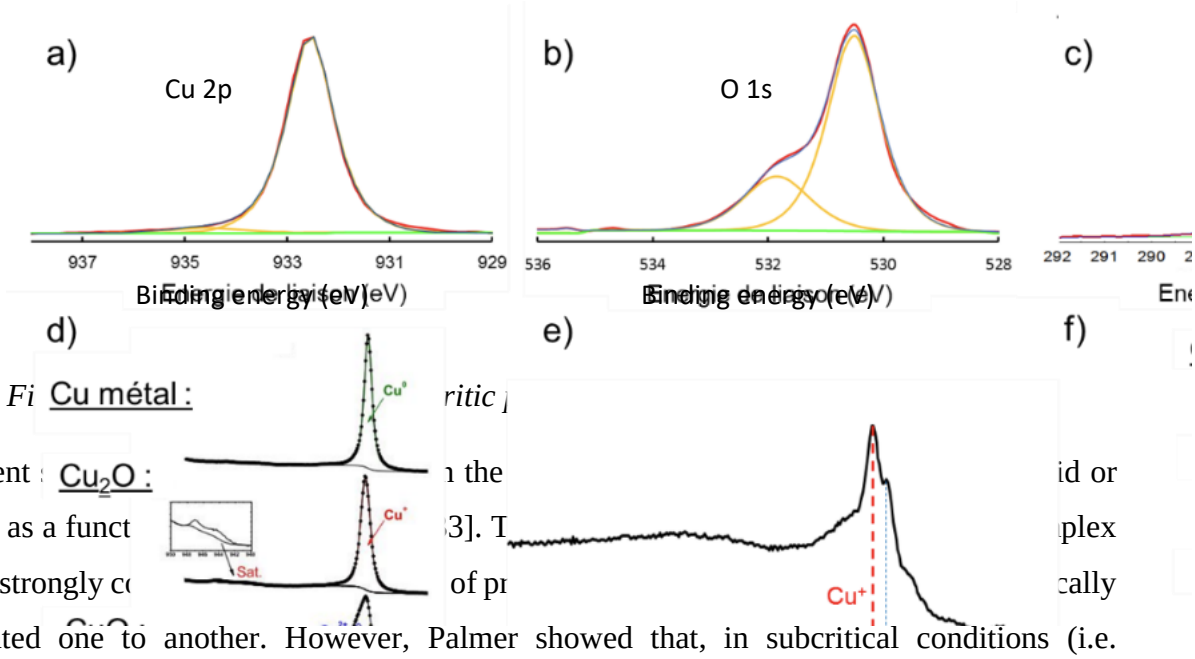

Fi *ritic*

Different ... the ... id or steam) as a funct ... 3]. T ... plex as it is strongly c ... of pr ... cally correlated one to another. However, Palmer showed that, in subcritical conditions (i.e. temperature and pressure do not simultaneously exceed Tc = 374.15 °C and Pc = 22.12 MPa, respectively) the solubility of cuprous oxide in water increased from room temperature to about 250-260 °C before decreasing when the starting pH is either neutral or acidic [31]. Moreover, the solubility of Cu_2O increased with increasing pressure to supercritical conditions ($T \geq$ 374.15 °C and $P \geq$ 22.12 MPa) but, for a given pressure, this solubility decreased with temperature above 200 °C [32]. These observations could be related to the behavior of the Cu/40CF MMC. First, the disappearance of the cuprite peak in the XRD pattern corresponds actually to the solubilization of this layer as the sintering temperature increases. Second, the

improvement of the densification, i.e. the dissolution-precipitation mechanism, could be related to the higher dissolution of Cu (Cu_2O) as $T_{sinter.}$ increases up to 265 °C. Then the sintered density decreases as the solubilization process decreases. One should notice that many works have evidenced that hydrothermal conditions are not detrimental to CF. For example, tetragonal $BaTiO_3$ has been synthesized in hydrothermal conditions (T= 225 °C in presence of KOH) using CF as support in order to enhance electromechanical coupling. Here no degradation of the microstructure of the CF is observed [34], however a surface activation of the fibres can be probably considered. In this way, it seems reasonable to consider that only copper species are reactive to dissolution-precipitation process.

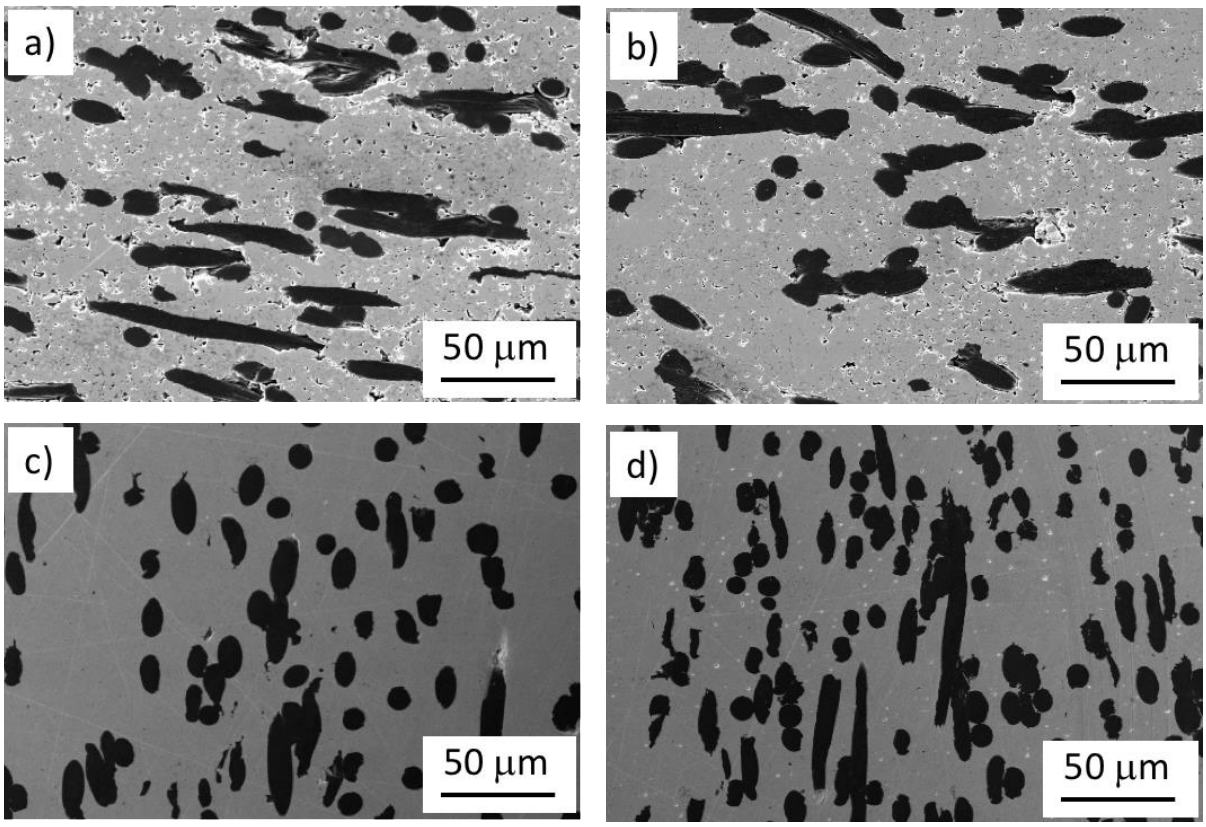

Figure 7: Microstructure of Cu/40CF MMC sintered during 180 min at 125 MPa at different sintering temperatures ($T_{sinter.}$): (a) 100 °C, (b) 180 °C, (c) 265°C and (d) 355 °C

Micrographs presented in Fig. 7 clearly show the improvement of densification as the sintering temperature increases up to 265 °C (from (a) to (c)). For the highest sintering temperature, $T_{sinter.}$ = 355 °C, the presence of remaining porosities (Fig. 3d) is in agreement with the decrease of the relative density (Table 2). No interface reaction between Cu and CF and neither

decomposition nor debonding of CF from the copper matrix was observed in the whole temperature range studied, at that scale of observation. Sintering of Cu/40CF in subcritical hydrothermal conditions above 200 °C appears to be beneficial in order to obtain high density MMC.

3.1.2 Influence of applied pressure

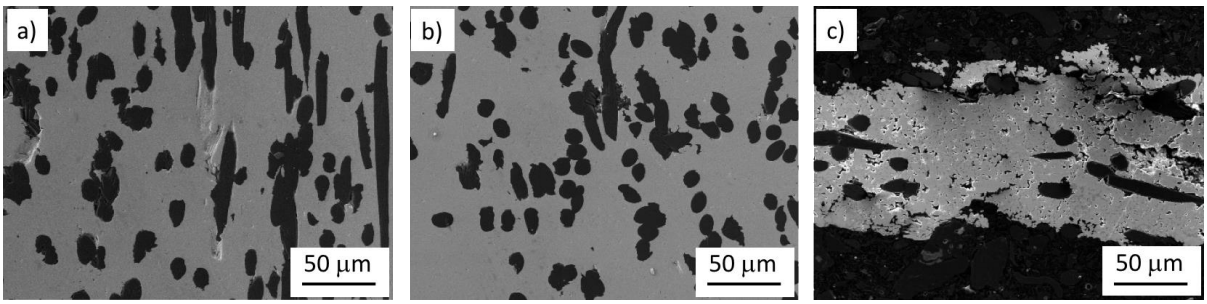

Figure 8: Microstructure evolution of Cu/40CF MMC sintered at 265 °C for 60 minutes at (a) 70 MPa (CC11) (b) 125 MPa (CC6) and (c) 250 MPa (CC7)

Applied pressure is a major parameter in the sintering of a green body. Hence, it is important to clearly identify the role of the applied pressure in HS. For this study, different pressures of densification (70 MPa, 125 MPa, 250 MPa) were applied at the beginning of the HS process (at room temperature: RT) and stay constant all along the process (rise in temperature and sintering step at $T_{sinter.}$). Considering that the dissolution/precipitation process is the dominant densification mechanism, an increase of the applied pressure leading to a driving force increase, through enhanced stress gradient, should improve densification. Surprisingly, the density of the sintered MMC did not increase with increasing pressure conditions, as it can be observed in Table 2. More precisely, when the applied pressure was increased from 125 MPa to 250 MPa, the composite density was dramatically reduced from 97% down to 73%. On that point, Figure 8 clearly shows the presence of large pores within the Cu/40CF MMC sintered under 250 MPa, compared to the one sintered at 125 MPa. Nevertheless, as pointed out previously in table 1, the external pressure can induce large plastic deformations, even at room temperature. Actually, previous work have shown that microcrystalline copper exhibited at room temperature a plastic deformation of 10 % after 5 hours for a stress flow of 200 MPa [35]. And, it took, for similar deformation, far less than 1 s second for a stress flow of 300 MPa [25]. This mechanical behavior suggests that important plastic deformation occurs when the applied pressure reaches 250 MPa, even at room temperature. Thus, plastic deformation and

dissolution/precipitation process are competitive mechanisms during HS of copper. A way to reduce the impact of plastic deformation without affecting the dissolution/precipitation process, is to decrease the applied pressure from 250 MPa to 125 MPa during the temperature increase (CC8 experiment, Table 2). The high density obtained ($d_{rel.}$ = 100%) clearly highlights the competiveness of the two involved densification mechanisms, and in addition that a high degree of plastic deformation annihilates the efficiency of the dissolution/precipitation mechanism for densification.

3.1.4 Influence of sintering time

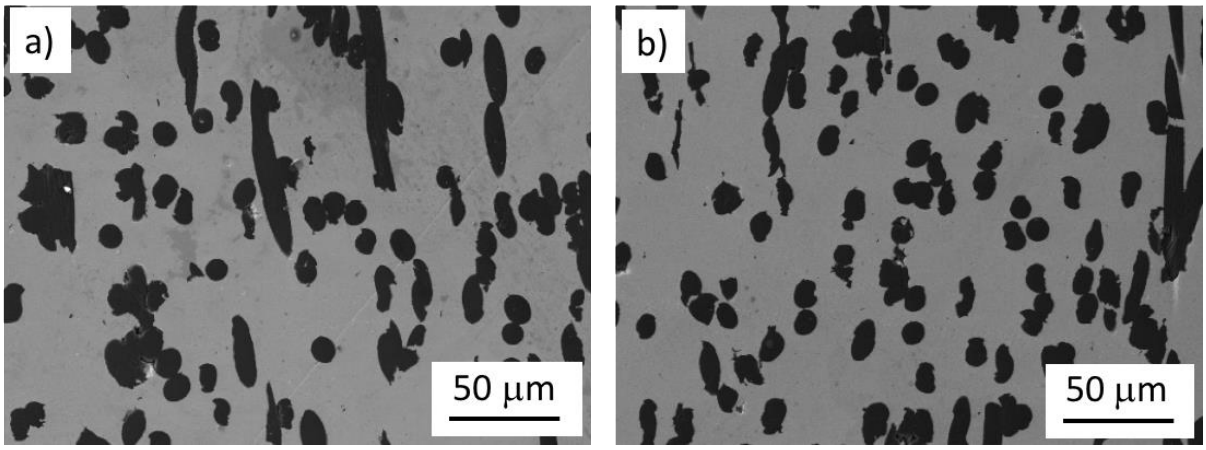

Figure 9. Microstructure of Cu/40CF MMC sintered at 265 °C under 250 MPa with 5wt% of water with a sintering time $t_{sinter.}$ of (a) 60 min and (b) 480 min

Sintering time ($t_{sinter.}$) is another parameter that is often used to adjust the density or the microstructure of sintered compacts. The effect of two sintering durations was investigated. Figure 9 (a) and (b) shows Cu/40CF MMC sintered at $T_{sinter.}$ = 265 °C, under $P_{sinter.}$ = 250 MPa (P_{start} = 125 MPa) for 60 and 480 min, respectively. Both the microstructure (Fig. 5) and the density of these samples ($d_{rel.}$ = 100%, Table 2) remained identical and high, respectively, whatever the sintering time. Also, no physical degradation of the CF is observed. It means that the densification process is already finished after 60 min.

3.2 Comparison of hot pressed and hydrothermal sintered Cu/40CF material properties

Hot pressing (HP) is a widely used technique for the fabrication of Cu/C composites. High densities can be achieved, but it leads to a preferential orientation of CF in a plane perpendicular to the loading direction and a random orientation of CF within this plane. Due to the fact that CF has anisotropic thermal conductivity (TC) properties (TC parallel to the axis

fiber equals to 540 W/m.K and TC perpendicular equals to 10 W/m.K), the resulting hot pressed MMC shows anisotropic macroscopic thermal conductivity. TC of hot pressed Cu/40CF in a plane perpendicular to the pressure direction is much higher than TC measured in a plane parallel to the pressure direction [36-42]. This is what was obtained for the HP1 sample, as shown in Table 3: $TC_{\perp}$ = 260 W/mK while $TC_{//}$ = 180 W/mK. The thermal properties of the hydrothermal sintered Cu/40CF samples were different. A smaller anisotropy was observed for the CC8 sample (240 vs 200 W/mK for $TC_{\perp}$ and $TC_{//}$, respectively) and an almost isotropic behavior was obtained for CC9 and CC10 MMC (~ 300 W/mK).

Table 3: Thermal conductivity (TC), coefficient of thermal expansion (CTE) and mechanical hardness (H_v) of sintered Cu/40CF and Cu samples

Sample code	**Sintering process**	**TC (W/mK) at 70 °C**		**CTE (10^{-6}/K)**		**Hardness (Hv)**
		Perpendicular	Parallel	Perpendicular	Parallel	
HP1 (Cu/40CF)	HP	260 ± 5	180 ± 4	10.0 ± 0.4	15.0 ± 0.5	55 ± 3
CC8 (Cu/40CF)	HS	240 ± 5	200 ± 4	10.2 ± 0.4	14.5 ± 0.5	58 ± 3
CC9* (Cu/40CF)	HS	300 ± 6	290 ± 6	8.1 ± 0.3	13.3 ± 0.5	63 ± 3
CC10* (Cu/40CF)	HS	298 ± 6	296 ± 6	8.3 ± 0.3	13.2 ± 0.5	65 ± 3
Cu powder	HS	370 ± 7	370 ± 7	17.2 ± 0.7	17.2 ± 0.7	52 ± 3
Cu powder	HP	390 ± 8	390 ± 8	18.1 ± 0.7	18.1 ± 0.7	-

Perpendicular: Perpendicular to the pressure direction; Parallel: parallel to the pressure direction

* : CIP pre-treatment at 200 MPa during 5 min, water being added after (CC9) or before (CC10) CIP

The microstructures of fractured Cu/40CF MMC, sintered by HP and HS respectively, are presented in Fig. 10 (a) and (b). CF appeared to be less aligned in the HS sintered sample (CC9) as many fibers are pointing perpendicular to the observation plane. It means that the orientation of CF in a plane perpendicular to the loading pressure is less favored for hydrothermal sintering. It can be related to the generation of an autogenous pressure within the compact due to the presence of water during HS. Moreover, when the sample is pre-compacted, using CIP, it leads to an isotropic distribution of CF in the Cu matrix (Fig. 3) that is maintained during HS, which explains the isotropic thermal properties, measured for these samples (CC9 and 10). It also means that densification is not only driven by plastic deformation of copper, but rather by the

dissolution/precipitation process specifically involved in the HS. Fig. 10 shows SEM micrographs of the CF before MMC fabrication and after MMC fabrication and Cu dissolution inside proper acid solution. Global diameter and length have not or just slightly change leading to the conclusion that the CFs have not been damaged by the HS process.

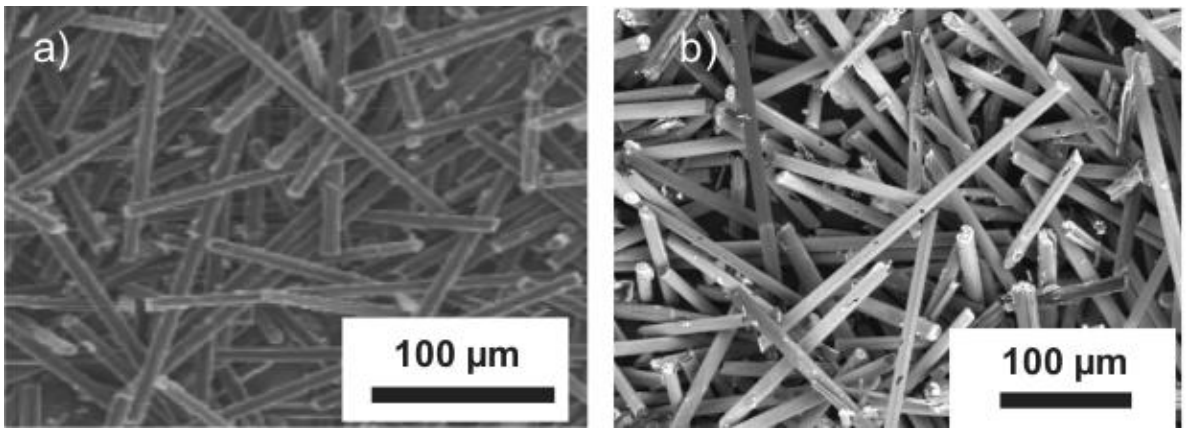

Fig10: SEM micrographs of CF a) before sintering process and b) after HS sintering process and Cu acid dissolution

Other physical properties of the sintered samples such as coefficient of thermal expansion (CTE) and mechanical hardness (H_v), are reported in Table 3. Cu/40CF samples sintered by HS have better properties (lower CTE in both parallel and perpendicular directions and higher H_v) than the one densified by HP. These properties are highly related to the interfacial bonding existing between CF and the copper matrix and the more random orientation of the CF for the HS composite materials. It is well known that no chemical bonding exists between pure Cu and C. The transfer of property between the CF and the matrix (that allows lowering the CTE of the HP Cu/40CF sample, compared to pure Cu) is due to the mechanical adhesion induced by the difference of CTE between the matrix and the reinforcement, during the cooling of the material. HS Cu/40CF samples present even lower CTE than HP's one. The only way to obtain such a good value is the formation of a chemical bonding between CF and Cu. It is in agreement with the dissolution/precipitation mechanism that needs chemical reaction at interfaces and allows matter transfer during sintering.

The improvement of the Vickers Hardness of the HS samples, compared to HP sample, can also be related to the microstructure of the copper matrix, which looks finer than HP's one. Therefore, the effect of the HS on a Cu powder alone was investigated. Sintering conditions were the same than Cu/40CF MMC (T_s = 265 °C, $P_{sinter.}$ = 250 MPa, 5 wt.% of water). Dense

compacts were obtained: $d_{rel.}$ = 100% (Table 3) with a homogeneous and fine microstructure. This first observation unambiguously confirms the sensitivity of copper species to dissolution-precipitation processes. Moreover, the thermal conductivity of this HS Cu sample (TC = 370 W/mK) almost reached the value of pure HP sintered copper of 390 W/mK. The slightly lower value may be related to the smaller grain size observed in HS sample, which corresponds to a larger number of grain boundaries that lower the thermal conductivity of the material. As for TC, CTE of Cu powder, sintered by HS, is nearly equivalent to that of a reference sintered Cu. The same trend is also observed for hardness measurements (Table 3. So, for pure copper, HS allows obtaining a high densification associated to a fine microstructure, which result in physical properties as good as other Cu pieces sintered at much higher temperatures. This is another example of the interest of HS, which combine applied pressure and transfer of matter trough dissolution-precipitation mechanisms.

3.3 Proposition of sintering mechanisms for HS

From the HS experimental results obtained in the present work, we can propose a representative diagram of the different sintering pathways of Cu/40CF materials (Fig. 11). As it has been pointed out in Table 1, the uniaxial pressure applied on the material induces stress gradients within Cu grains that are the driving force for two densification mechanisms, the thermoplastic deformation and the dissolution-precipitation process involving the liquid phase and thus specificities of hydrothermal conditions. Thus, the prevalence of one mechanism or the other depends on the experimental conditions used (pressure, temperature).

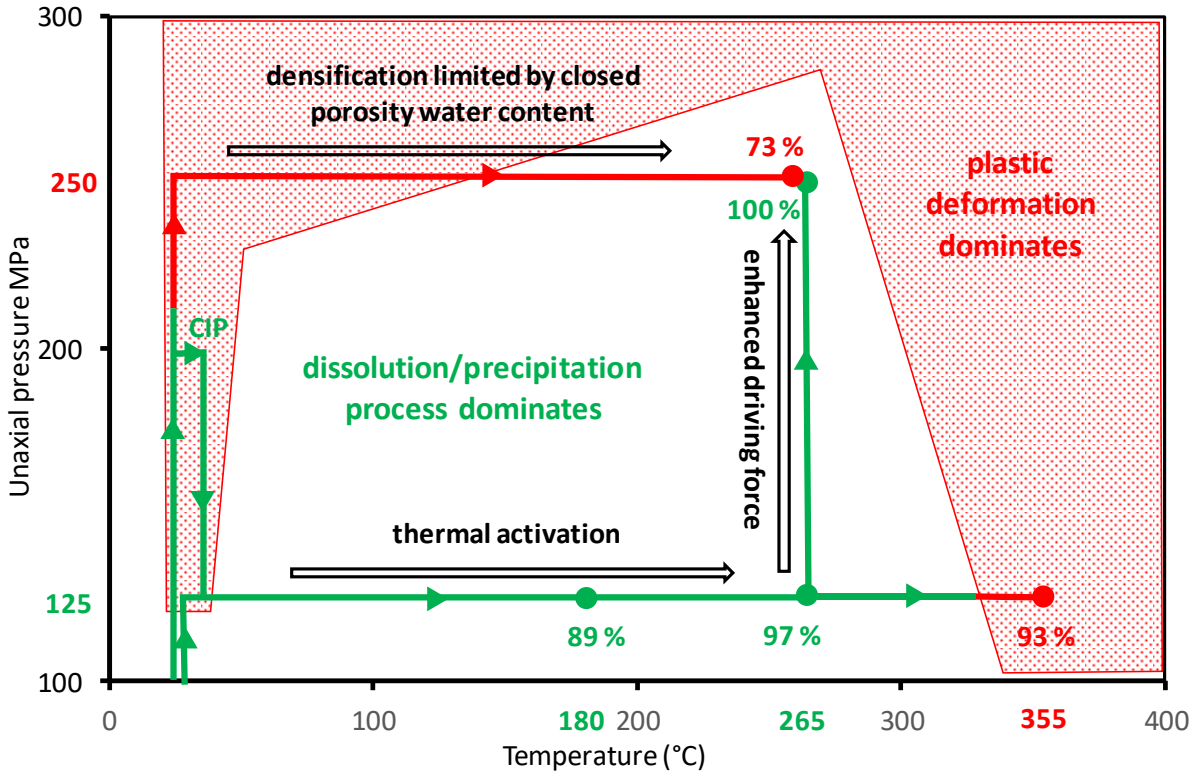

Figure 11: Schematic P-T diagram showing the sintering pathways to achieve dense MMC (green lines) or low-density MMC (red lines), for a sintering time of 60 min, in relation with the dominant mass transport mechanism.

At room temperature, when the initial cold pressing is performed, only plastic deformation can occur. No copper, nor copper oxide dissolution in water is observed for times less than days or months [29]. Depending on the pressure used, the microstructure of the cold pressed compact can change a lot. On the one hand, at high pressure (250 MPa), the formation of close porosity is occurring, leading to entrapment of water within these pores. Then, heating leads to the creation of an internal pressure likely to oppose to the densification process. Also, there is no extended accessible area to promote dissolution-precipitation of copper. This is why low final densities (73%) were finally obtained. On the other hand, cold pressing at lower pressure lets the presence of open porosity within the material and the possibility to develop dissolution-precipitation phenomena, as the temperature increases. In that conditions, matter transport is efficient, and a 100% relative density is obtained for the same sintering parameters (P=250 MPa, T_s = 265 °C) but with a low-pressure pathway (Fig. 8). In the P-T domain where the dissolution/precipitation process dominates, thermal activation or enhanced driving force allow to increase MMC density. Now, insofar as solubility of copper species decreases above ~ 250 °C and plastic deformation is thermally activated, the plastic deformation mechanism becomes

predominant at high temperature. It corresponds to the observed density decrease (CC1 sample) when the sintering temperature goes from 265 °C to 355 °C (P = 125 MPa). This is supported by previous works concerning compressive stress-strains results for pure copper: at 400 °C, 100% of deformation can be obtained very rapidly (less than 15 min) at a pressure close to 125 MPa [43,44].

This schematic shows that the dissolution-precipitation process has to be the dominant sintering mechanism to achieve high densification. It should be added that the hydrothermal conditions used also avoid a planar orientation of CF in a plane perpendicular to the pressing direction which could be related to the creation of small autogenous pressure during sintering.

4. Conclusion

Copper matrix composites is one of the widely used engineering materials for their high thermal and electrical conductivities. They are also widely explored for heat sink applications that requires high thermal conductivity and low thermal expansion co-efficient. The currently existing fabrication methods involve use of high temperatures for consolidating as dense materials. The high temperatures employed in the classically used hot pressing methods softens and reinforcement materials such as carbon fibers are used for enhancing their thermal stability. The uniaxial pressure applied during the fabrication process by hot pressing creates anisotropic thermal properties. In the present work, we proposed an innovative low temperature high pressure technique called as hydrothermal sintering to sinter full density Copper/40Carbon fiber MMC at 265°C and 250 MPa in presence of water. We are first in the literature to report on MMC material sintering by hydrothermal sintering. Various sintering parameters were studied for optimizing the best conditions for sintering Copper/40Carbon fiber MMC. The optimized parameters of hydrothermal sintering for Copper/40Carbon fiber is P = 250 MPa; T_S = 265 °C; t= 60 min and water quantity = 5 wt.%. The results obtained clearly emphasize the potential of hydrothermal sintering as a clean technique that can be successfully employed for fabrication of MMC. The dissolution and precipitation mechanisms were identified, and the role of water exhibited in the form high density samples. The hydrothermal sintering Copper/40Carbon fiber MMC yielded improved thermal and thermo-mechanical properties and is isotropic in terms of their thermal properties, this is another major highlight of the present study. To increase the reactivity between the copper and carbon fiber, change of surface of

carbon fiber and increased reaction time in hydrothermal regime can create a pathway to create interfacial interaction between Cu and CF.

5. Acknowledgments

(Late) Prof. Gérard DEMAZEAU, who passed away on 3rd November 2017 is fondly remembered for his contributions to hydrothermal activities at ICMCB.

6. References

[1] Qu X, Zhang L, Wu M, Ren S. Review of metal matrix composites with high thermal conductivity for thermal management applications. Prog. Nat. Sci. Mater. Int. 2011; 21: 189-197. doi:10.1016/S1002-0071(12)60029-X.

[2] Carbon Fibre Reinforced Copper Matrix Composites: Production Routes and Functional Properties. Microstructural Investigation and Analysis, Volume 4 - Buchgraber - Wiley Online Library. http://onlinelibrary.wiley.com/doi/10.1002/3527606165.ch22/summary.

[3] Surappa MK. Aluminum matrix composites: Challenges and opportunities. Sadhana. 2003; 28: 319-334. doi:10.1007/BF02717141.

[4] Sheng J, Wang L, Li S, Yin B, Liu X, Fei WD. Phase-Transformation-Induced Extra Thermal Expansion Behavior of $(Sr_xBa_{1-x})TiO_3$/Cu Composite. Sci. Rep. 2016; 6:27118. doi:10.1038/srep27118.

[5] Neubauer E, Kitzmantel M, Hulman M, Angerer P. Potential and challenges of metal-matrix-composites reinforced with carbon nanofibers and carbon nanotubes. Compos. Sci. Technol.2010; 70:2228-2236. doi:10.1016/j.compscitech.2010.09.003.

[6] Dash K, Ray BC, Chaira D. Synthesis and characterization of copper–alumina metal matrix composite by conventional and spark plasma sintering. J. Alloys Compd. 2012; 516:78-84. doi:10.1016/j.jallcom.2011.11.136.

[7] Silvain JF, Vincent C, Heintz JM, Chandra N. Novel processing and characterization of Cu/CNF nanocomposite for high thermal conductivity applications. Compos. Sci. Technol. 2009; 69:2474-2484. doi:10.1016/j.compscitech.2009.06.023.

[8] Mayerhofer KE, Neubauer E, Eisenmenger-Sittner C, Hutter H. Adhesion promotion of Cu on C by Cr intermediate layers investigated by the SIMS method. Anal. Bioanal. Chem. 2002; 374:602-607. doi:10.1007/s00216-002-1540-3.

[9] Mortimer DA, Nicholas M. The wetting of carbon and carbides by copper alloys. J. Mater. Sci. 1973; 8:640-648. doi:10.1007/BF00561219.

[10] Mortimer DA, Nicholas M. The wetting of carbon by copper and copper alloys. J. Mater. Sci. 1970; 5:149-155. doi:10.1007/BF00554633.

[11] Ullbrand JM, Córdoba JM, Tamayo-Ariztondo J, Elizalde MR, Nygren M, Molina-Aldareguia JM, Odén M. Thermomechanical properties of copper–carbon nanofibre composites prepared by spark plasma sintering and hot pressing. Compos. Sci. Technol.2010; 70:2263-2268. doi:10.1016/j.compscitech.2010.08.016.

[12] Vakifahmetoglu C, Anger JF, Atakan V, Quinn S, Gipta S, Li Q, Tang L, Riman RE. Reactive Hydrothermal Liquid-Phase Densification (rHLPD) of Ceramics – A Study of the BaTiO3[TiO2] Composite System. Journal of the American Ceramic Society 2016; 99(12):3893-3901. doi/10.1111/jace.14468/abstract

[13] Guo H, Baker A, Guo J, Randall CA. Protocol for Ultralow-Temperature Ceramic Sintering: An Integration of Nanotechnology and the Cold Sintering Process. ACS Nano.2016; 10:10606-10614. doi:10.1021/acsnano.6b03800.

[14] Guo J, Guo H, Baker AL, Lanagan MT, Kupp ER, Messing GL, Randall CA. Cold Sintering: A Paradigm Shift for Processing and Integration of Ceramics. Angew. Chem. 2016; Int. Ed. 55:11457-11461. doi:10.1002/anie.201605443.

[15] Guo J, Guo H, Baker AL, Randall CA. Hydrothermal-Assisted Cold Sintering Process: A New Guidance for Low-Temperature Ceramic Sintering - ACS Applied Materials & Interfaces 2016; 8, 32:20909-20915. http://pubs.acs.org/doi/abs/10.1021/acsami.6b07481.

[16] Guo H, Baker A, Guo J, Randall CA. Cold Sintering Process: A Novel Technique for Low-Temperature Ceramic Processing of Ferroelectrics. Journal of the American Ceramic Society (2016); 99(11): 3489-3507. doi/10.1111/jace.14554/abstract

[17] Baker A, Guo H, Guo J, Randall C. Utilizing the Cold Sintering Process for Flexible–Printable Electroceramic Device Fabrication. Journal of the American Ceramic Society (2016); 99(10):3202-3204. doi/10.1111/jace.14467/abstract

[18] Bouville F, Studart AR. Geologically-inspired strong bulk ceramics made with water at room temperature. Nat. Commun. 2017; 8:14655. doi:10.1038/ncomms14655

[19] Yamasaki N, Yanagisawa K, Nishioka M, Kanahara S. A hydrothermal hot-pressing method: apparatus and application. Journal of Materials Science Letters. 1986; 5:355-356. doi:10.1007/978-94-009-0743-0_70

[20] Goglio G, Largeteau A, Ndayishimiye A, Prakasam M. Procédé et dispositif de densification des matériaux ou de consolidation d'un assemblage de matériaux par frittage hydrothermal ou solvothermal. French Patent Application FR17 /54585 (May 2017)

[21] Ndayishimiye A, Largeteau A, Mornet S, Duttine M, Dourges MA, Denux D, Verdier M, Gouné M, Hérisson de Beauvoir T, Elissalde C, Goglio G. Hydrothermal Sintering for Densification of Silica. Evidence for the Role of Water. J. Eur. Ceram. Soc. 2018; 38:1860-1870. doi:10.1016/j.jeurceramsoc.2017.10.011

[22] Ndayishimiye A, Largeteau A, Prakasam M, Pechev S, Dourges MA, Goglio G. Low temperature hydrothermal sintering process for the quasi-complete densification of nanometric α-quartz. Scr. Mater. 2018; 145 :118-121. doi:10.1016/j.scriptamat.2017.10.023.

[23] Ndayishimiye A., Buffière S., Dourges M.A., Largeteau A., Prakasam M., Mornet S., Kaman O., Zdenek J., Hejtmanek J., Goglio G., Design of 0-3 type nanocomposites using hydrothermal sintering, Scr. Mater. 2018; 148: 15-19. doi:10.1016/j.scriptamat.2018.01.013.

[24] Goglio G., Ndayishimiye A., Largeteau A., Elissalde C., Viewpoint on hydrothermal sintering: main features, today's recent advance and tomorrow's promises, Scr. Mater. (2018). doi:10.1016/j.scriptamat. 2018.08.038.

[25] Al Baida H, Langlade C, Kermouche G, Ambriz RR. Identifying the stress-strain curve of materials by micro-impact testing. Application on Aluminum alloy 6061-T651, pure Copper and pure Iron. J. Mater. Res. 2015; 30 2222-2230. Doi.org/10.1557/jmr.2015.186

[26] Savitskii AP, Zhdanova VN, Girya ÉN. The effect of sintering temperature on the strength of powder copper subjected to repeated pressing. Sov. Powder Metall. Met. Ceram. 1964; 3:311-315. doi:10.1007/BF00774176

[27] Beverskog, B., Puigdomenech, I. Revised Pourbaix diagrams for copper at 25 to 300°C. J. Electrochem Soc. 1997; 144:3476–3483

[28] Feng Y, Teo WK, Siow KS, Tag KL, Hsieh AK. the corrosion behaviour of copper in neutral tap water. part I: corrosion mechanisms. Corrosion Sci. 1996; 38:369-385

[29] Hultquist G, Szaka´los P, Graham M. J, Belonoshko A. B, Sproule G. I, Grasjo L, Dorogokupets P, Danilov B, AAstrup T, Wikmark G, Chuah G.-K, Eriksson J.-C, Rosengren A. Water Corrodes Copper. Catal Lett. 2009; 132:311–316. Doi 10.1007/s10562-009-0113-x

[30] Zhou P, Hutchison M.J, Scully J.R, Ogle K. The anodic dissolution of copper alloys: Pure copper in synthetic tap water. Electrochimica Acta 2016; 191:548–557

[31] Palmer D, Bénézeth P. Solubility of Copper Oxides in Water and Steam, 14th Int. Conf. Prop. Water Steam Kyoto. 2004; 491–496.

[32] Palmer D. Solubility measurements of crystalline Cu_2O in aqueous solution as a function of temperature and pH. J Solution Chem. 2011; 40:1067–1093. Doi 10.1007/s10953-011-9699-x

[33] Palmer D, The solubility of crystalline cupric oxide in aqueous solution from 25°C to 400°C. J. Chem. Thermodynamics 2017; 114:122–134

[34] Bowland C.C, Sodano H.A. Hydrothermal synthesis of tetragonal phase $BaTiO_3$ on carbon fiber with enhanced electromechanical coupling. J. Mater. Sci. 2017; 52:7893–7906.

[35] Champion Y, Langlois C, Guérin-Mailly S, Langlois P, Bonnentien JL, Hÿtch MJ. Near-Perfect Elastoplasticity in pure Nanocrystalline Copper. Science 2003; 300:310-311. doi: 10.1126/science.1081042

[36] Geffroy PM, Chartier T, Silvain JF. Preparation by tape casting and hot pressing of copper carbon composites film., J. Eur. Ceram. Soc.2007; 27:291-299. doi:10.1016/j.jeurceramsoc.2006.04.054.

[37] Guillemet T, Geffroy PM, Heintz JM, Chandra N, Lu Y, Silvain JF.,An innovative process to fabricate copper/diamond composite films for thermal management applications. Compos. Part Appl. Sci. Manuf.2012; 43:1746–1753. doi:10.1016/j.compositesa.2012.04.015

[38] Couillaud S, Lu YF, Silvain JF. Thermal conductivity improvement of copper–carbon fiber composite by addition of an insulator: calcium hydroxide. J. Mater. Sci. 2014; 49:5537-5545. doi:10.1007/s10853-014-8246-8.

[39] Veillère A, Heintz JM, Chandra N, Douin J, Lahaye M, Lalet G, Vincent C, Silvain JF. Influence of the interface structure on the thermo-mechanical properties of Cu–X (X=Cr or B)/carbon fiber composites. Mater. Res. Bull. 2012; 47:375-380. doi:10.1016/j.materresbull.2011.11.004

[40] Lalet G, Kurita H, Heintz JM, Lacombe G, Kawasaki A, Silvain JF. Thermal expansion coefficient and thermal fatigue of discontinuous carbon fiber-reinforced copper and aluminum matrix composites without interfacial chemical bond. J. Mater. Sci. 2014; 49:397-402. doi:10.1007/s10853-013-7717-7.

[41] Lalet G, Kurita H, Miyazaki T, Kawasaki A, Silvain JF. Thermomechanical stability of a carbon fiber-reinforced aluminum matrix composite fabricated by spark plasma sintering in various pulse conditions. Mater. Lett. 2014; 130:32-35. doi:10.1016/j.matlet.2014.05.070

[42] Geffroy PM, Mathias JD, Silvain JF. Heat Sink Material Selection in Electronic Devices by Computational Approach. Adv. Eng. Mater. 2008; 10:400-405. doi:10.1002/adem.200700285

[43] Manonukul A, Dunne FPE. Initiation of dynamic recrystallization under inhomogeneous stress states in pure copper. Acta Mater. 1999; 47:4339-4354.

[44] Huang SH, Shu DY, Hu CK, Zhu SF. Effect of strain rate and deformation temperature on strain hardening and softening behavior of pure copper. Trans. Nonferrous Met. Soc. China 2016; 26:1044-1054.